Wind Tunnel Analysis of the Detachment Bubble on Bolund Island

T S Yeow[1, 3], **A Cuerva**[1], **B Conan**[2] **and Pérez-Álvarez**[1]**, J.**
[1]IDR/UPM, E.T.S.I. Aeronáuticos, Universidad Politécnica de Madrid, E-28040 Madrid, Spain
[2]von Karman Institute, Rhode-Saint-Genèse Belgium

E-mail: teeseong.yeow@upm.es

Abstract. The flow topology on two scaled models (1:230 and 1:115) of the Bolund Island is analysed in two wind tunnels, focusing on the characteristics of the detachment pattern when the wind blows from 270º wind direction and the atmospheric condition is neutral. Since the experiments are designed as the simplest possible reference cases, no additional roughness is added neither to the models surface nor to the wind tunnel floor. Pressure measurements on the surface of the 1:230 scale model are used to estimate the horizontal extension of the intermittent recirculation region, by applying the diagnostic means based in exploring the pressure statistics, proposed in the literature for characterising bubbles on canonical obstacles. The analysis is done for a range of Reynolds numbers based on the mean undisturbed wind speed, U_∞ and the maximum height of the island, h [5.1×10^4, 8.5×10^4]. An isoheight mapping of the velocity field is obtained using 3D hotwire (3D HW). The velocity field in a vertical plane is determined using 3D HW and 2D particle image velocimetry (PIV) on the 1:115 scale model in order to reproduce and complete already existing results in the literature.

1. Introduction

Recently, the Bolund experiment (see [1], [3], [4]) has been proposed as the new test case for benchmarking of numerical and physical modelling of complex terrain flows. The Bolund experiment was initiated by Risø-DTU as a blind comparison of different numerical models (including linear, RANS and LES simplifications of Navier-Stokes equations). The main conclusions from the initial analysis are: *a*) a great scatter of the numerical results exist (mainly in the vicinity of the island escarpment, *b*) the mean velocities are better predicted than turbulent kinetic energy (TKE), and *c*) the best models predicting both, mean wind speed and TKE are the RANS models with two closure equations, see [3] and [14].

One of the main geometric characteristics of the Bolund Island is the escarpment facing approximately the wind directions 200º to 295º (see figure 1, center). It can be idealised as a combination of a 50º ramp extending from the sea level to 0.5*h*, plus an almost vertical step from 0.5*h* to *h*, being *h* the total height of the escarpment. The escarpment height varies slightly in the interval 200º-295º being roughly the maximum height of the island (11.73 m). This geometry guarantees that flow detaches at the edge (with a sufficiently large Reynolds number) while the flat top ensures reattachment of the flow on the island. This flow pattern has been evidenced by smoke visualizations in wind tunnel in [1], quantified

[3]To whom any correspondence should be addressed.

by real scale measurements of reversed flow and very high values of TKE in the met masts close to the escarpment for heights below 2 m (met masts M2 and M6 for 239º and 270º wind directions respectively, see figure 1-right and [1] for met mast coding) and by Lidar scanning in [8], and indirectly by surface pressure measurements in wind tunnel in [16] and [17].
In previous works, [16], [17], the authors have analysed the detachment pattern at the Bolund escarpment by exploring the statistics of the surface pressure field. For this purpose, existing studies on canonical obstacles such as those on blunt flat plates with right-angled corners (BFP, see, for instance, [9] and [10]) and forward-facing steps with right-angled corners (FFS, see for instance [10] and [13]) were used as references. Several conclusions on the fluid dynamic process taking part in the detachment-reattachment region have been established from these studies (see [5], [9] and [10]). Also, the averaged topology of the recirculation region, mainly its averaged horizontal extension, has been correlated with the basic set of parameters characterising the inflow, such as the Reynolds number based on the free stream velocity and the obstacle height, Re_h, the ratio δ/h (being δ the boundary layer thickness), the ratio between the longitudinal integral length scale and the obstacle height, ${}^{x}L_u/h$, and, finally, the longitudinal turbulence intensity, I_u. These studies on canonical geometries have also established relations between the averaged location of the reattachment point and the location of some singular points of the surface pressure statistic field, such as the point where the mean pressure coefficient presents its maximum slope, the point where the coefficient of the pressure standard deviation is maximum or the point where the skewness of the pressure becomes positive (see [16]).
In this paper, the referred surface pressure study is used as a reference for a direct velocimetry analysis of the flow topology on a 1:115 scale model of the Bolund Island. The paper is organised as follows: the experimental set-up is described in section 2. In section 3, a characterisation of the reference boundary layers in the used wind tunnels is presented. New velocity measurements for the line B case for a 270º wind direction (see figure 1-right, [1], [2] and [3] for explanation) and transects at 2 m and 5m heights are analysed and compared with previous scaled and real measurements in section 4. In section 5, the basic statistics of the velocity field, obtained by traversing a 3D HW at a constant distance from the island surface is shown. In section 6, the velocity field along line B a 270º wind direction is analysed using 2D PIV. Finally, conclusions are presented in section 7.

2. Experimental set-up

Both mock-ups have been manufactured by computer aided manufacturing utilising the same topography data file used by the numerical modellers during the blind test experiment (see [1]). This file has been also used to program the iso-height traversing of the 3D HW (see below).
The surface pressure tests have been carried out on a 1:230 model of the Bolund island, in the A9 wind tunnel of IDR-UPM (Instituto Ignacio da Riva-Universidad Politécnica de Madrid) which is an open circuit suction type Eiffel wind tunnel with a closed test chamber. The convergent section of the wind tunnel is bi-dimensional with a length of 5.25 m and an input section of 4.8 m wide and 1.8 m high. The test chamber has the following dimensions: Length: 3 m × Width: 1.5 m × Height: 1.8 m. The wind tunnel is driven by nine eight-bladed variable speed fans with nominal output of 10 kW capable of producing winds of 5-35 m/s. The mounting of the model is made using a turntable installed in the sidewall of the test section of the wind tunnel. (See figure 1-center and [16]). The pressure measurements were recorded at a rate of 100 Hz over 180 s for each pressure tab. The measurements for all the pressure tabs were done in 2 measurement blocks of 256 pressure tabs with 12 reference pressure tabs always present in each block. A pitot tube was installed upstream of the model to measure the instantaneous static pressure and the instantaneous total pressure. For a more detailed description of the pressure measurement set-up, see [16].
The 3D HW and 2D PIV tests have been performed in a 1:115 scale model of the Bolund Island in the ACLA16 wind tunnel, which belongs to the same institution, see figure 1-left. The ACLA16 WT is also an open circuit suction type Eiffel wind tunnel with a closed test chamber of 2.2 m wide and 2.2 m high. The convergent section of the wind tunnel is bi-dimensional with a length of 6.0 m leading

into a straight test section of 18 m allowing the natural development of the boundary layer. The wind tunnel is driven by sixteen eight-bladed variable speed fans with nominal output of 7.5 kW capable of producing winds up to 30 m/s. A dedicated traversing system has been installed allowing the displacement of a sensor in a volume of 2.2 m×1.5 m×1 m with a precision of 10^{-5} m.
The hotwire system is a DANTEC Streamware set-up with four constant temperature anemometers (CTAs) channels. A DANTEC 3D HW probe (55P91 with 1.25 mm active length wires) has been used to simultaneously measure the three components of wind speed vector above the model. The 55P91 probe has been mounted on the appropriate support and automatically traversed to map the iso-height lines and surfaces above the model of the island. The sampling frequency varies from 2 kHz up 8 kHz and the sampling time from 16 s up to 130 s depending on the application.
The PIV system is a 2D one from TSI Inc. A Nd-YAG laser with a power of 200 mJ/pulse, emitting a laser beam with a wavelength of 532 nm is used to illuminate the flow. The flow field image is captured with a 2048 x 2048 pixels CCD camera with a maximum frame rate of 15 fps. The camera is positioned along the wall of the wind tunnel test section at a focus distance of roughly 0.8 m. The size of the image frame is in the region of 0.2 m×0.2 m and the capture rate is set at 4 fps. Sebacate particles with a size of roughly 1-3 μm were generated using a Laskin nozzle and released as tracer particles. A total of 10 frames were captured along the whole length of the model along the 270º line. Displacement markers were used before each capture to allow the matching of the images after processing. A set of 1000 images were captured for each frame to allow the averaging for the mean values. The PIV images were processed using a 64x64 pixels initial interrogation window with a final window of 32x32 pixels (roughly 3x3mm window resolution). This gives a vector field with less than 7% outliers which were then replaced using the appropriate post-processing technique [12].

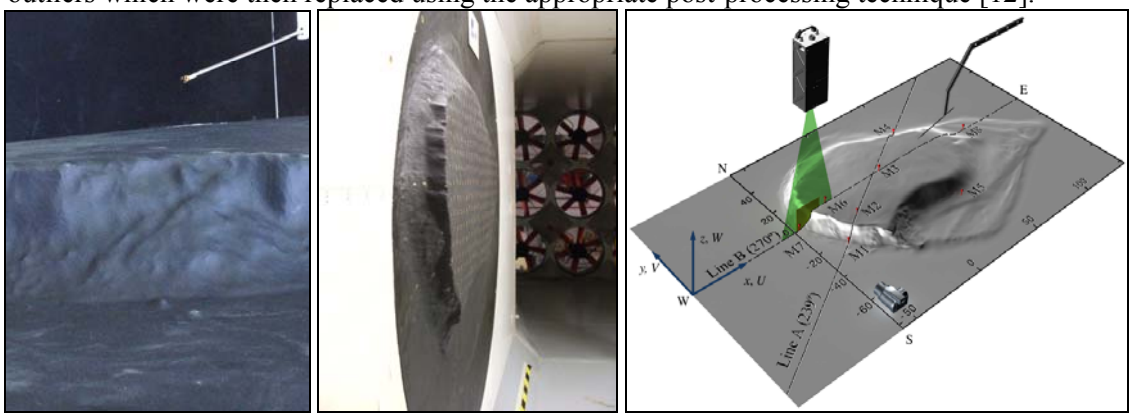

Figure 1: Left: Traversing of the 3D HW probe on the 1:115 scale Bolund model in the ACLA16 wind tunnel. Center: Pressure test on the 1:230 scale model in the A9 WT seen from the 270º direction. Right: PIV and HW systems setups in the ACLA16 WT and Bolund references.

3. Analysis of the reference wind conditions

The boundary layers of both wind tunnels have been explored using 1D HW anemometry in the case of the A9 WT and 3D HW and also 2D PIV in the case of the ACLA16 WT. The main BL characteristics of the A9 WT are described in [16]. The ACLA16 wind tunnel has a boundary layer thickness, $\delta = 0.22$ m, a longitudinal turbulence intensity in the free stream, I_u=1.75 % and the integral length scale of the longitudinal wind velocity component in the longitudinal direction is ${}^{x}L_u = 0.35$ m. The characteristics of the ACLA16 boundary layer measured approximately 0.3 m upstream of the location of the Bolund model (measured before its installation) using 3C HW are shown in Table 1 and figure 2, where the vertical profile of the mean velocity and the longitudinal turbulence intensity are presented, and in figure 3, where the vertical profile of the mean velocity, standard deviation of longitudinal and vertical components of wind velocity, and the correlation of both fluctuations

components are shown in plus units. The values obtained are compared with the results from [6] for smooth conditions and [7] for smooth and transitionally rough conditions, suggesting that the conditions of the present test are likely transitionally rough which is coherent with the values of the friction Reynolds number based in the aerodynamic roughness length, z_0, showed in Table 1.

Table 1. Main characteristics of the ACLA16 boundary layer. U_δ, is the mean velocity at 0.99δ, θ is the momentum thickness, Re_θ is the Reynolds number based in θ and U_δ, u_τ is the friction velocity, and z_0 is the aerodynamic roughness length. Measured with 3D HW.

	U_δ [ms^{-1}]	δ [m]	θ [m]	Re_θ	u_τ[ms^{-1}] *a*/*b*[a]	z_0 [m] *a*/*b*[b]	$u_\tau\, z_0\, \nu^{-1}$
Case 1	7.5	0.22	0.02	10000	0.277/0.293	1.08×10^{-5} / 0.717×10^{-5}	0.212
Case 2	15.1	0.21	0.018	18000	0.534/0.572	0.54×10^{-5} / 0.367×10^{-5}	0.205

[a] *a*: calculated from *uw* correlation, *b*: calculated from the log profile.

[b] *a* : calculated from the log profile. *b*: calculated as $z_0 = 0.14\nu/u_\tau$. See [15].

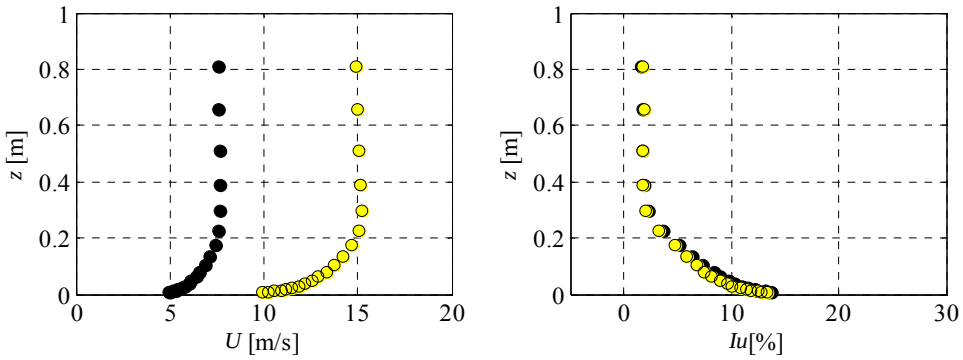

Figure 2: *Left*: Mean speed profile of the boundary layer in the ACLA16. *Right*: Longitudinal turbulence intensity profile in the ACLA16. Legend: ● : Re_θ=10000, ○ : Re_θ=18000. Measured with 3D HW.

4. Line B transects at 2 m and 5 m heights

The normalized mean velocity magnitude $S(x,z)/S_0(z)$ and the normalized increase of TKE, $\Delta k(x,z)$ as proposed in [3] are presented in figure 4 for direction 270º (line B in figure 1-right, [3]) at $y = 0$ and at two constant heights, 2 m and 5 m (full scale) above ground level (a.g.l.). $S(x,z)$ is the mean velocity magnitude at a given longitudinal position x and height z a.g.l. over the island, and $S_0(z)$ is the corresponding undisturbed inflow value at the same height a.g.l. The normalized increase of TKE is defined as $\Delta k(x,z)=[k(x,z)-k_{05}]/S_0(z)$, where $k(x,z)$ is the TKE at a longitudinal position x and height z a.g.l. and k_{05} is the corresponding undisturbed inflow value at a scaled height corresponding to z=5 m a.g.l. at full scale. The data have been measured for a Re_h = 51500 and a ratio δ/h = 2.2. The scaled experimental results provided in the context of the Bolund blind comparison are also shown (they are identified by "Other WT" in the figure) along with the real scale measurements from the ultrasonic anemometers at the corresponding heights in met masts M7, M6, M3 and M8 (they are identified by "Sonics" in the figure).

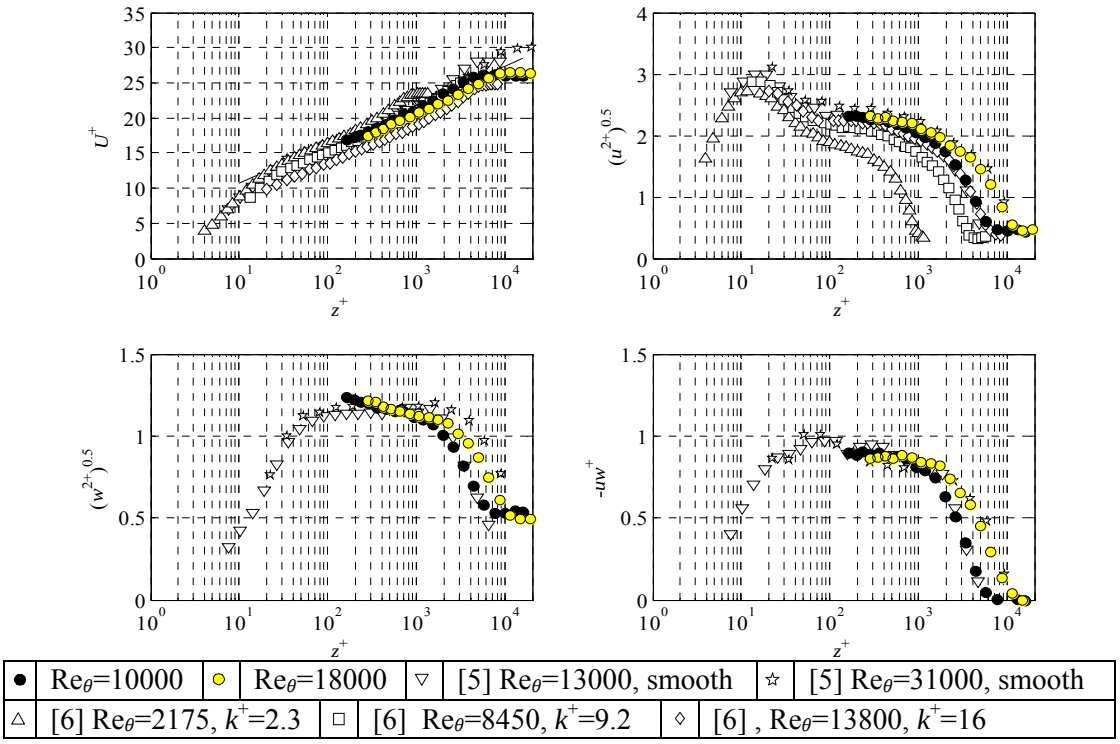

●	Re_θ=10000	○	Re_θ=18000	▽	[5] Re_θ=13000, smooth	☆	[5] Re_θ=31000, smooth
△	[6] Re_θ=2175, k^+=2.3	□	[6] Re_θ=8450, k^+=9.2	◇	[6] , Re_θ=13800, k^+=16		

Figure 3: Vertical profiles in plus units (+) of: *Top left*: Mean speed, *Top right*: Standard deviation of the longitudinal component of wind velocity. *Bottom left*: standard deviation of the vertical component of wind velocity. *Bottom right*: covariance of the longitudinal and vertical components of wind velocity. k^+ is the roughness Reynolds number based in the equivalent sandgrain roughness length. Measured with 3D HW.

The new measurements of S/S_0 are quite similar to the previous scaled results. The over-speeding predicted is quite similar in the wake (lee side) of the island both for 2 m and 5 m, and slightly larger (10% of the free wind speed more) in the flat part of the island. The over-speeding peak for all scaled measurements is quite above the full scale measurement for the 2 m case. Most of the computational models also predict (see [14], as an example) a much larger over-speeding at this point. Some reasons can be anticipated for this disagreement between scaled and full scale results. The first one being a lack of fidelity in the reproduction of the edge sharpness which leads to higher mean speeds and lower levels of TKE after the scaled escarpment, second a matter of the scales, so the full scale flow behaves in a different way. For the 5 m transect, the new measurements of S/S_0 agree quite well with the measurements from the ultrasonic anemometer in M6 location. The wind tunnel measurements in the blind comparison results and the current results both predict a larger over-speeding along the flat region on the top of the island. The blockage factor is lower than the allowable 5%, therefore blockage is unlikely to be the cause of this mismatch. Another possible reason could be the lower levels of roughness that are reproduced in the mock-up or the already mentioned lack of fidelity in the reproduction of the edge.

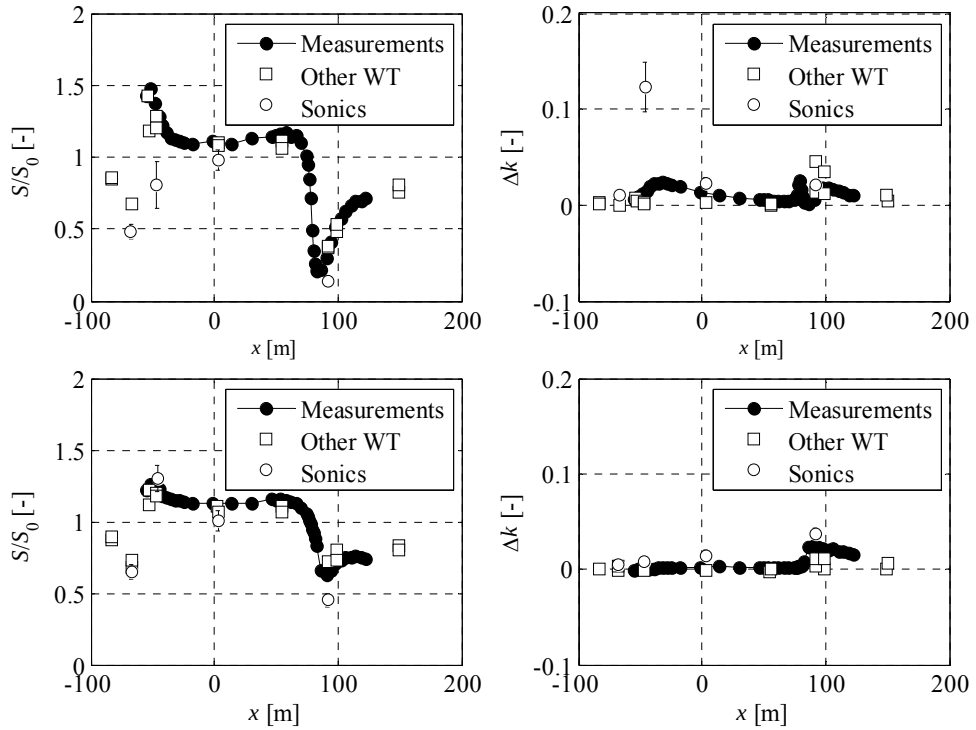

Figure 4: *Left*: Speed-up, S/S_0. *Right*: Normalized increase of TKE, Δk. The top row shows the results corresponding to 2 m a.g.l., while the bottom row corresponds to 5 m a.g.l. Line B for a 270º wind direction. Re_h = 51500. Measured with 3D HW.

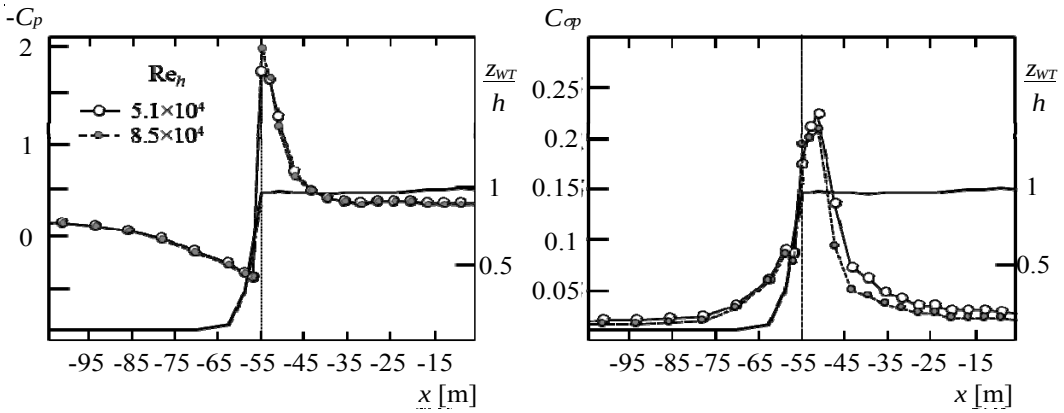

Figure 5: *Left*: Distribution of mean pressure coefficients along the line B for a 270º wind direction. *Right*: Standard deviation of the surface pressure coefficients along the same line. From [16] and [17].

Regarding the normalized increment of TKE, Δk, all scaled measurement under-predict the values compared to the real scale test, likely meaning that the real island introduces more energy in the large scales of the real flow than in the scaled cases. The under-prediction of the peak of Δk in the detachment region (around M6) exhibited by the scaled measurement at 2 m a.g.l. could be explained by the same causes responsible of the over-prediction of S/S_0 already commented. It is remarked that the high number of measurement points in the new experiment has allowed identifying specific patterns in both of S/S_0 and Δk, especially in the detachment region at the front and in the wake region (lee side). These patterns are qualitatively reproduced by some of the computational models tested in the Bolund blind experiment [2]. It is remarked that the hotwire measurements at the wake of the

island, especially at 2 m, requires a consistency analysis with PIV data since in this region the presence of an intermittent recirculation pattern is very likely. This crosscheck analysis is being performed by the authors but is not presented here since it is out of the scope of the current work. Figure 5 shows the distribution of negative mean pressure coefficient, $-C_p$, and standard deviation of the surface pressure coefficient, $C_{\sigma p}$, along line B for a 270º wind direction. Highly negative values of power coefficient as well as high values of its standard deviation, are found at the escarpment edge, what can be considered as indirect symptoms of a likely detachment flow pattern.

5. Horizontal mapping of the velocity field

The capabilities of the traversing system have been exploited to map the velocity field at a constant height of 5 m a.g.l. with 3D HW anemometry. Each mapping point is horizontally spaced out 0.04 m at model scale which translates to 4.6 m at full scale. The speed-up, S/S_0 and the normalized increase of TKE, Δk, as seen in figure 4 are plotted in figure 6 along with the negative of the mean pressure coefficient, $-C_p$, on the surface and the standard deviation pressure coefficient, $C_{\sigma p}$, on the surface.

The horizontal mapping of the velocity magnitude gives a quick overview of the flow behaviour over the Bolund Island. The 3D pattern of the flow over the island is clearly visible from the mapping. It is clear that the 2D insight of the flow obtained from the measurements along the transect lines does not give a true characteristic of the 3D flow over the terrain. Along the transect Line B, the flow is modified as would a flow over a 2D step qualitatively be. However, on both sides of the center line, the 3D effect introduced by the Bolund Island modifies the flow creating a low speed region. This 3D pattern is also present in the TKE plot of the mapping of the Bolund Island, where two stream-wise regions of higher Δk have been detected, most probably originated by the horizontal shear layer between the central higher speed region and the two lateral regions with lower speed. The influence of the escarpment geometry on this TKE pattern is currently being analysed by the authors.

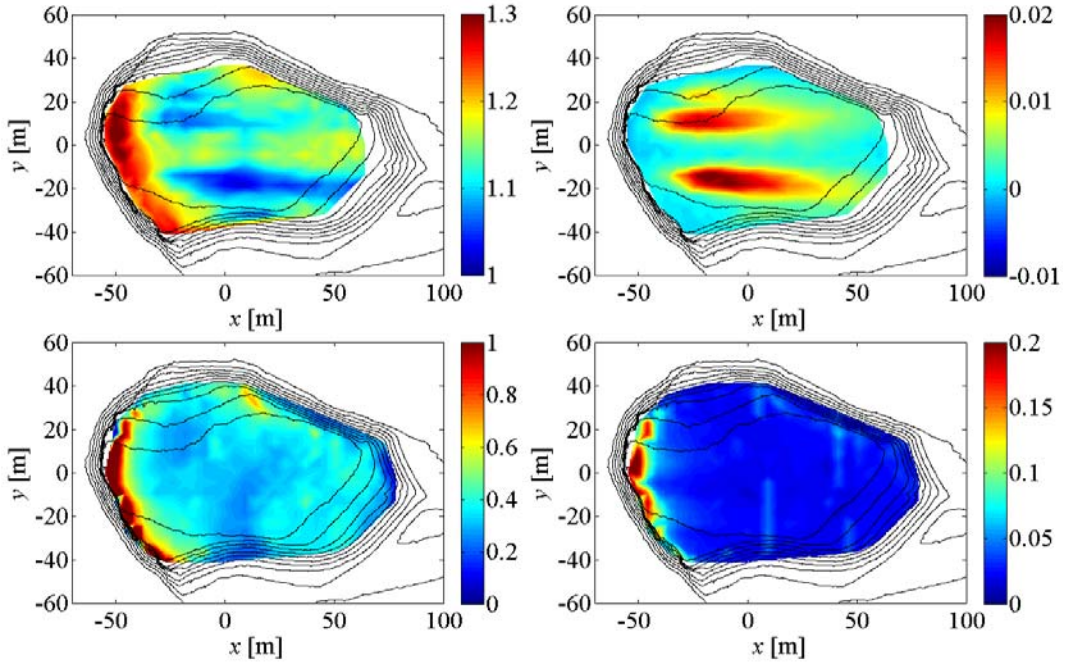

Figure 6: *Top left*: Speed-up, S/S_0, at 5.0 m a.g.l. *Top right*: Normalized increase of the TKE, Δk, at 5.0 m a.g.l., Measured with 3D HW. *Bottom left*: Surface distribution of the negative of the mean pressure coefficient, $-C_p$. *Bottom right*: Standard deviation of the surface pressure coefficient, $C_{\sigma p}$,. Re_h = 51500 for top figures and Re_h = 51000 for bottom figures. 270º wind direction

There is a clear correspondence of the high speed region and the highly negative pressure coefficient region at the escarpment edge.

6. Vertical mapping of the velocity field

Utilising 2D PIV, the vertical mapping of the intermittent recirculation pattern over the island has been measured and visualised for the line B and 270º wind direction. The escarpment in front of the Bolund Island acts as a step which modifies the mean flow as can be seen in figure 7, where a low speed region forms at the front of the escarpment. On the top of the island, close to the ground, the low speed region observed at full scale is not being detected neither by the 2D PIV (possible reasons for this mismatch have already been proposed). A high speed region can be observed above this last region and close to the escarpment in agreement with the full scale measurements. In figure 8, one shot of the instantaneous velocity vectors and an instantaneous color map of the horizontal velocity component are shown. On the left side, an instantaneous recirculation pattern present in front of the island is shown while on the right side, an instantaneous shot of the intermittent recirculation process on the top of the island is presented.

The probability of occurrence of negative values of the instantaneous horizontal velocity is presented in figure 9 and gives an indication on where the most probable location of reverse flow takes place. The probability is calculated as the ratio of occurrences of negative values of the instantaneous horizontal velocity on the total number of instantaneous values in a given point (1000). This result allows the estimation of the extension, likelihood and intensity of the recirculation pattern. The results shown in the plot agree with the results of the surface pressure measurements in figure 5 (see [16]) where the intermittent reattachment region on the top of the island is identified by the rough coincidence of the region with non-zero probability of recirculation on the top of the island, and the region where the standard deviation pressure coefficient peaks.

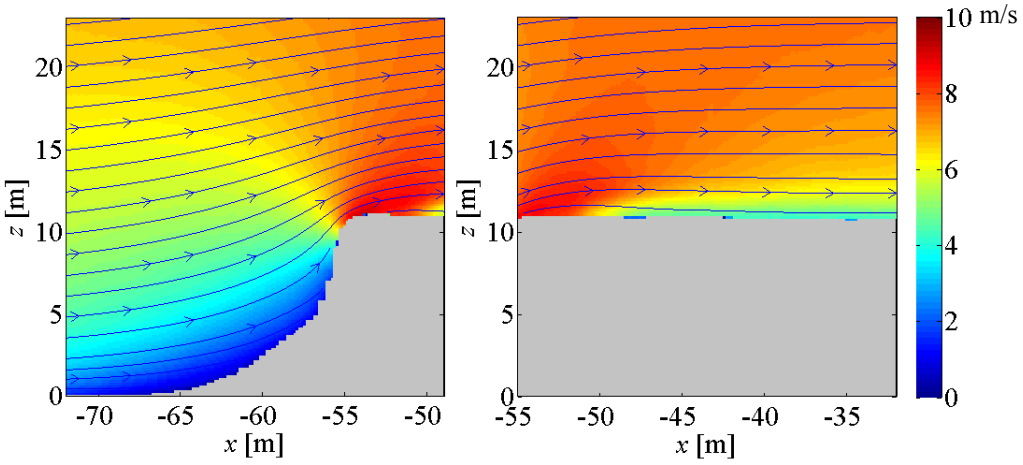

Figure 7: Mean velocity magnitude [m/s], averaged over 1000 vector fields, along the line B for a 270º wind direction over the front escarpment of the Bolund model. The blue arrows show the mean streamlines of the flow over the Bolund model. The results are obtained from 2D PIV images therefore only *U* and *W* components are considered. Re_h = 51500.

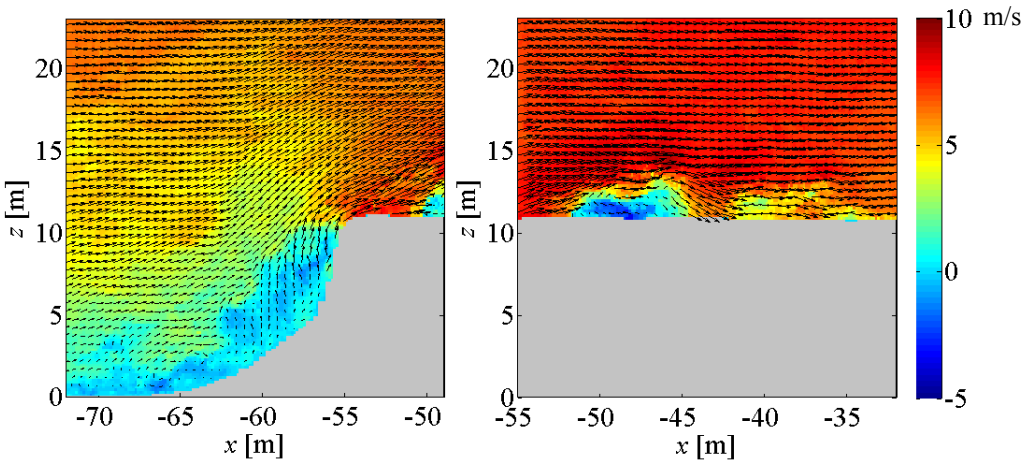

Figure 8: Instantaneous velocity field (vectors) and instantaneous horizontal component of the velocity [m/s] (color map) along the line B for a 270º wind direction over the front escarpment of the Bolund model. Both frames were taken at different instances. The results are obtained from 2D PIV. Re_h = 51500.

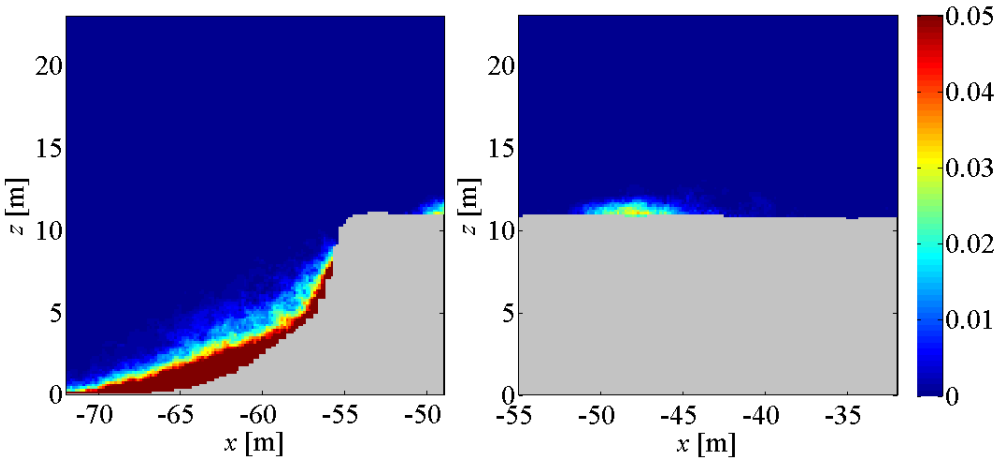

Figure 9: Probability of occurrence of instantaneous negative horizontal velocity component in a set of 1000 PIV images along the line B for a 270º wind direction over the front escarpment of the Bolund model. Re_h = 51500.

7. Conclusions

The flow over a scaled model of the Bolund Island was analysed using surface pressure measurements, 3D hotwire anemometry and 2D particle image velocimetry. Combining these different techniques, some characteristics of the flow were obtained and compared with other wind tunnel and full scale results. The mapping of the Bolund Island using 3D hotwire and automated traversing provided a visualization of flow behaviour over the model revealing a highly three dimensional pattern. Combining with 2D PIV measurements, an estimation of the longitudinal extension of the intermittent recirculation pattern on top of the escarpment was obtained, showing that the prediction of the intermittent reattachment point from pressure measurements agreed with the direct 2D PIV visualization.

8. References

[1] Bechmann, A., Berg, J., Courtney, M.S., Joergensen, H.E., Mann, J., Soerensen, N.N. 2009. The Bolund Experiment: Overview and Background Risoe-R-1658(EN).
[2] Bechmann, A. 2010. Presentations from "The Bolund Experiment Workshop" 3-4th December 2009 Risoe-R-1745(EN).
[3] Bechmann A, Sørensen NN, Berg J, Mann J, Réthoré P-E (2011) The Bolund experiment, part II: blind comparison of microscale flow models. Boundary-Layer Meteorology 141, 245-271.
[4] Berg J, Mann J, Bechmann A, Courtney MS, Jørgensen HE. The Bolund experiment, part i: flow over a steep, three-dimensional hill. Boundary-Layer Meteorology 2011; 141(2): 219–243. DOI:10.1007/s10546-011-9636-y.
[5] Bradshaw, P., Wong, F. 1972. The reattachment and relaxation of a turbulent shear layer. Journal of Fluid Mechanics 52, 113.
[6] DeGraff, D, Eaton, J. K. 2000. Reynolds-number scaling of the flat-plate turbulent boundary layer. Journal of Fluid Mechanics 422, 319-346.
[7] Schultz, M. P., Flack, K. A., 2007. The rough-wall turbulent boundary layer from the hydraulically smooth to the fully rough regime. Journal of Fluid Mechanics 580, 381-405.
[8] Mann J, Angelou N, Mikkelsen T, Hansen KH, Cavar D, Berg J. Laser Scanning of a Recirculation Zone on the Bolund Escarpment. The Science of Making Torque from Wind, October, 9-11, Oldenburg, 2012.
[9] Kiya, M., Sasaki, K. 1983. Structure of a turbulent separation bubble. Journal of Fluid Mechanics 137, 83-113.
[10] Largeau, J.F., Moriniere, V. 2007. Wall pressure fluctuations and topology in separated flows over a forward-facing step. Experiments in Fluids 42, 21-40.
[11] Nakamura, Y., Ozono, S. 1987. The effects of turbulence on a separated and reattaching flow. Journal of Fluid Mechanics 178, 477-490.
[12] Raffel M, Willert C, Wereley S, Kompenhans J. Particle Image Velocimetry. A Practical Guide. 2ed. Springer-Verlag, 2007.
[13] Tachie, M., Balachandar, R., Bergstrom, D. 2001. Open channel boundary layer relaxation behind a forward facing step at low Reynolds numbers. Journal of fluids engineering 123, 539-544.
[14] Prospathopoulos, J.M., Politis, E.S., Chaviaropoulos, P.K. 2012. Application of a 3D RANS solver on the complex hill of Bolund and assessment of the wind flow predictions. Journal of Wind Engineering and Industrial Aerodynamics 107-108, 149-159.
[15] Yeow, T.S., Cuerva, A., Pérez, J., Conan, B., Buckingham, S., von Beeck, J. 2010. Modelling of atmospheric *boundary layer*: Generation of shear profile in wind tunnel. 6th PhD Seminar on Wind Energy in Europe 2010.
[16] Yeow, T.S., Cuerva, A., Pérez, J. 2011. Pressure Measurement of the Detachment Bubble on the Bolund Island. Proceeding of PHYSMOD 2011, Hamburg.
[17] Yeow, T.S., Cuerva, A., Pérez, J. 2012. Pressure Measurement of the Detachment Bubble on the Bolund Island. Proceedings of EAWE 2012 Annual Event, Copenhagen.

Acknowledgments

This work was carried as part of the WAUDIT project within the FP7 Marie-Curie Initial Training Network.